Journal of Alloys and Compounds 504S (2010) S410–S413

Contents lists available at ScienceDirect

Journal of Alloys and Compounds

journal homepage: www.elsevier.com/locate/jallcom

Evolution of texture and microstructure in pulsed electro-deposited Cu treated by Surface Mechanical Attrition Treatment (SMAT)

Romain Blonde[a], Hoi-Lam Chan[b], Nathalie Allain-Bonasso[a], Bernard Bolle[c], Thierry Grosdidier[a], Jian Lu[b,*]

[a] LETAM, CNRS 3143, Université Paul Verlaine-Metz, Ile du Saulcy, 57045 Metz, France
[b] The Hong Kong Polytechnic University, Hung Hom, Kowloon, Hong Kong
[c] LETAM, Ecole Nationale d'Ingénieurs de Metz, Ile du Saulcy, 57045 Metz, France

ARTICLE INFO

Article history:
Received 31 July 2009
Received in revised form 3 April 2010
Accepted 8 April 2010
Available online 15 May 2010

Keywords:
Coating materials
Nanostructured materials

ABSTRACT

This paper presents the microstructure and texture evolution in pulsed electro-deposited copper samples and the additional effect of the Surface Mechanical Attrition Treatment (SMAT), which were analyzed by means of electron backscattering and X-ray diffractions. A transition in the microstructure was observed as the thickness of the deposit increased: from randomly oriented equiaxed (3D) nanograins at the beginning of the deposition process towards elongated (2D) nanograins having a strong ⟨1 1 0⟩ fibre texture. Meanwhile, the SMAT treatment is shown to randomize the strong texture of the electrodeposits.

1. Introduction

Nanocrystalline (NC) and sub-microcrystalline metallic materials have been the subject of extensive investigations and nanostructured bulk materials have been produced by a number of processing methods including (i) severe plastic deformation of bulk microstructured materials such as high pressure torsion (HPT) [1], equal channel angular extrusion/pressing (ECAE/ECAP) [2,3] or accumulative roll-bonding (ARB) [4]; (ii) consolidation of nanostructured particles by cold pressing and/or extrusion [5,6], thermal/plasma spraying of thick deposits [7–9], and, more recently, techniques for which an electric current was used to aid the pressure assisted sintering [10,11]. However, the drawback of nanostructured bulk materials is their limited ductility of only a few percent of uniform elongation. For practical applications of nanostructured metals, it is therefore required to optimize the balance between strength and ductility. One of the methods is to tailor the grain size structure in order to get bimodal or multi-modal grain size distributions [12]. Even if the number fraction of larger grains in the nanostructure is low, their volume fraction can be sufficiently high to contribute to dislocation-based plasticity in the material [12]. Therefore, both thermo-mechanical and powder metallurgy approaches have been tested over the last years to produce this type of hybrid microstructures [12–16]. In many of the tested processes, the intrinsic heterogeneity of the recrystallisation process was used to introduce some large recrystallised grains within a heavily deformed structure. The difficulty however lies in the exact control of the thermo-mechanical sequence to generate the suitable mixture in a fairly reproducible manner [17]. An alternative method is also to exploit the specific nature of twin boundaries as a specific barrier to dislocations [18]. Nanoscale twins can be introduced during the process of pulsed-electro-deposition of Cu [19,20] and, with an increase of twin boundary density, both the tensile strength and the ductility were increased remarkably [21]. The texture developed in these pulsed-current electro-deposited samples has not been considered yet. This is however an interesting aspect because of (i) the intrinsic anisotropy of copper and (ii) the oriented twinning mechanism itself.

As the failure of the materials are very often triggered from the surface (fatigue, fretting, corrosion, wear, etc.), the optimization of the surface microstructure and properties is often an effective approach to enhance the global behavior and service lifetime of materials. The "Surface Mechanical Attrition Treatment" (SMAT) has recently merged as a powerful technique to create nanostructure at the top surface while hardening the material over a depth of several 100 of μm. SMAT induces a grain refinement through severe plastic deformation imparted at high strain rate to the material by balls [22,23]. The SMAT process has been successfully applied to various material systems including Cu [24], Ni [25], Ti [26], iron [27,28] and stainless steels [29,30]. Again, despite these numerous studies, no information is available on the texture modification

* Corresponding author at: Mechanical Engineering Department, The Hong Kong Polytechnic University, Hung Hom, Kowloon, Hong Kong. Tel.: +852 27666665; fax: +852 23647183.
E-mail address: mmmelu@inet.polyu.edu.hk (J. Lu).

0925-8388/$ – see front matter © 2010 Elsevier B.V. All rights reserved.
doi:10.1016/j.jallcom.2010.04.040

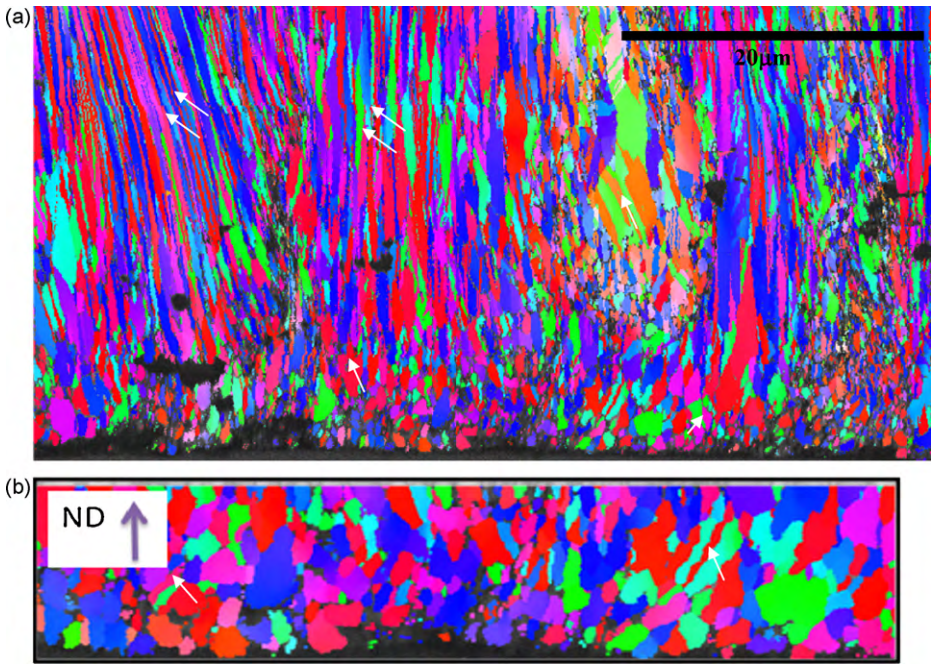

Fig. 1. EBSD images of the deposited sample: (a) lower part (next to the substrate) showing the equiaxed to columnar transition, (b) higher magnification of the equiaxed zones.

imparted in the surface due to the heavy deformation associated with the SMAT treatment.

This paper presents the first results of an on-going research study set-up to analyze the microstructure and texture evolution in electro-deposited copper samples and see the additional effect of the SMAT treatment.

2. Experimental procedure

The pure copper deposit was obtained by means of electro-deposition using an electrolyte of $CuSO_4$ solution with cathodic square wave pulses with an on-time of 0.2 ms and an off-time of 2 ms. The nominal peak current density was 1.5 A/dm^2. The substrate was wax which coated with silver conducting paints prior to the electroplating. Contrary to what was done in other studies where goal was to obtain ultra fine grains with different twin densities [19,21], the electro-deposition conditions were not optimized to increase the twin density. On the contrary, the fairly high on/out current ratio used here produced slightly larger grains with fewer twins that authorized a good EBSD characterization. A JEOL 6500F type field emission gun scanning electron microscope (FEG-SEM) equipped with an electron backscattering diffraction (EBSD) attachment was used to gain more information about the microstructure of the treated surface layers. For the EBSD analysis, the SEM was operated at 15 kV with the sample tilted by 70° and the step size was set at 30 nm. The texture analysis were carried out using an Inel diffractometer equipped with an Eulerian cradle and a Curve Position Sensitive Detector (Inel CPS120) able to cover 120° in 2θ.

3. Results and discussion

Fig. 1a shows an orientation imaging microscopy EBSD map from the bottom part of the deposit. The grains are represented with different colours while the substrate shows up with a dark contrast at the bottom of the image. The black areas present close to the substrate or within the deposit correspond to domains for which kikuchi bands could not be indexed (either absent or blurred). These were essentially domains where the material was preferentially removed during the electro-polishing procedure. This is for example the case in some locations along the substrate/deposit interface where the finest grains constructed at the early stages of the deposition process were removed. The part of the deposit along the substrate consists of a zone of fairly equiaxed grains that extends, depending of the local areas, over distances ranging from 5 to 15 μm. The equiaxed grains in this zone have sizes ranging from about 100 nm to 1 μm. A higher magnification of a local area in this zone is presented in Fig. 1b. As was confirmed by a detailed boundary misorientation analysis, the alternate change in colours (arrowed) indicates the presence of twins within some equiaxed grains. On top of this zone of equiaxed grains are gradually growing grains of higher aspect ratio. These grains are generally elongated towards the growth direction of the deposit. Ultimately, some of these grains can be 200 nm in diameter for a length of several tens of micron (double arrowed). This type of behaviour was verified on several deposits. There is a clear change during the growth of pulsed-electro-deposited materials from equiaxed (3D) nanograins towards the formation of elongated (2D) nanograins.

Fig. 2 gives results of the X-ray diffraction analysis showing the global texture at the beginning of the pulsed-current deposition process (analysis carried out after removing the substrate; Fig. 2a) and after several mm of growth (analysis on the top surface of the deposit; Fig. 2b). For each case, a set of two recalculated pole figures, namely the (2 0 0) and (2 2 0), is given. The pole figures in Fig. 2b clearly show a fibre texture with the ⟨1 1 0⟩ orientations parallel to the growth axis (i.e. the normal direction (ND) to the sample surface). This texture is fairly sharp. The maximum, at the centre of the (2 2 0) pole figure, reaches 8.9 mru (multiple of random unit) for a texture index of 6.6. Comparatively, the pole figures in Fig. 2a show a broad distribution of orientation. The maximum is at 2.7 mru for a texture index of 1.5 only. The occurrence of a ⟨1 1 0⟩ fibre texture when thickness increases is consistent with recent XRD studies of the texture development in copper deposits obtained by using continuous current [31–33]. In addition, our EBSD investigation clearly show a transition in the grain morphology when thickness increase. This indicates that the 3D nanograins formed at the beginning of the pulsed electro-deposition process are rather randomly oriented and that the elongated grains corresponds to a selective growth of the ⟨1 1 0⟩ oriented grains.

Fig. 3 gives the (2 0 0) and (2 2 0) recalculated pole figures obtained from the XRD analysis of the top surface of the pulsed deposited sample after the SMAT process. The strong ⟨1 1 0⟩ fibre texture (Fig. 2b) present at the end of the pulsed deposition has been

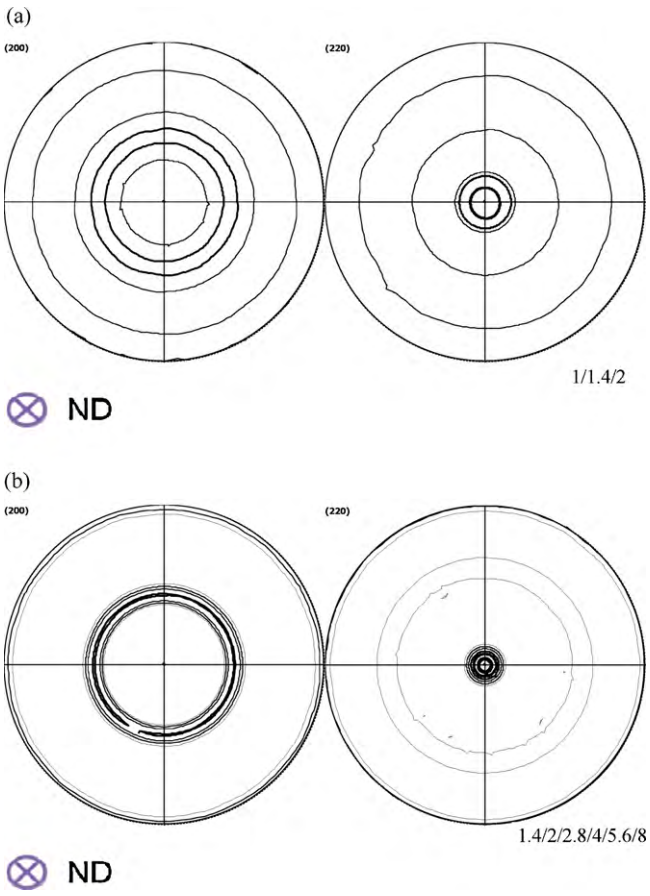

Fig. 2. Recalculated (2 0 0) and (2 2 0) pole figures from the bottom (a) and top (b) surfaces of the deposit.

reduced drastically after SMAT. The maximum, still at ⟨1 1 0⟩//ND, is now only at 3.4 mru and the texture index has dropped to 1.5. Microstructural evolution and grain refinement under SMAT have recently been investigated in pure coarse grain copper [24]. It was demonstrated that two different mechanisms took place depending on the levels of strain rate. In the subsurface layer of the SMAT Cu samples (deeper than 25 μm), at low strain rates, the grains were refined via the formation of dislocation cells. Comparatively, in the top surface layer (below 25 μm), the grain refinement mechanisms involved the additional formation of deformation nano-twins [24]. Fig. 4 gives a SEM image of the cross-section of the material in the SMATed area after strong etching. At the bottom part of the image,

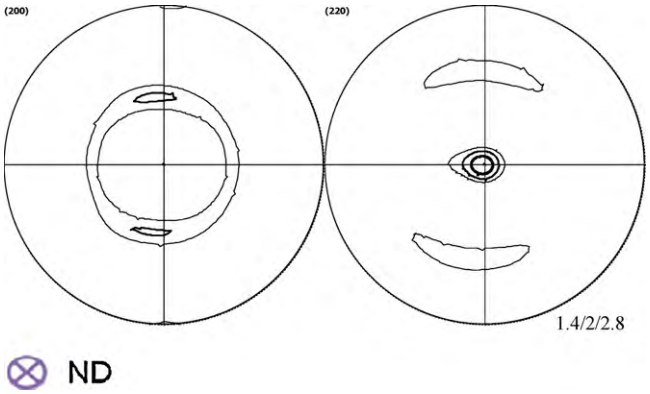

Fig. 3. Recalculated (2 0 0) and (2 2 0) pole figures from the top surface of the deposit after SMAT.

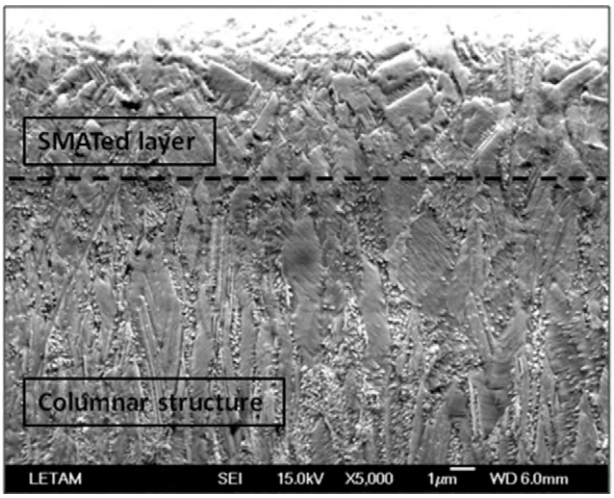

Fig. 4. SEM image of an etched electro-deposited sample after SMAT showing the presence of equiaxed grains at the top surface.

the etching reveals the columnar structure that build up during electro-deposition. Comparatively, equiaxed grains are present at the top surface that was subjected to the SMAT treatment. This suggests that, in the present case, some recrystallisation took also place under SMAT of this electro-deposited sample. The present analysis indicates that these mechanisms occurring during SMAT also involve a randomization of the strong texture created during the pulse electro-deposition.

4. Conclusion

(i) The analysis of the microstructure evolution in electro-deposited copper samples obtained under pulsed-current clearly revealed a transition from equiaxed (3D) nanograins towards the formation of elongated (2D) nanograins as the thickness of the deposit increases.
(ii) For the present deposition conditions, this transition took place at about 10–15 μm form the substrate.
(iii) The equiaxed (3D) nanograins formed at the beginning of the deposition process presented a fairly random texture. Comparatively, a strong ⟨1 1 0⟩ fibre texture characterized the areas where the elongated (2D) nanograins were retained.
(iv) The SMAT treatment is shown to randomize the strong texture created during the pulse electro-deposition. This is due to the occurrence of some recrystallisation.

Acknowledgement

The authors wish to acknowledge the financial support of Research Grants Council of Hong Kong Special Administrative Region of China under the PolyU7/CRF/08. The authors would also like to thank the editor and reviewers for their careful reading of the manuscript and constructive comments provided.

References

[1] R.Z. Valiev, R.K. Islamgaliev, I.V. Alexandrov, Prog. Mater. Sci. 45 (2000) 103–189.
[2] V.M. Segal, Mater. Sci. Eng. A 197 (1995) 157–164.
[3] R.Z. Valiev, T.G. Langdon, Prog. Mater. Sci. 51 (2006) 881–981.
[4] Y. Saito, H. Utsunomiya, N. Tsuji, T. Sakai, Acta Mater. 47 (1999) 579–583.
[5] D.G. Morris, M.A. Morris, Acta Metal. Mater. 39 (1991) 1763–1770.
[6] A.P. Newbery, B. Ahn, T.D. Topping, P.S. Pao, S.R. Nutt, E.J. Lavernia, J. Mater. Proc. Technol. 203 (2008) 37–45.
[7] T. Grosdidier, A. Tidu, H.L. Liao, Scripta Mater. 44 (2001) 387–393.
[8] J. He, J.M. Schoenung, Mater. Sci. Eng. A 336 (2002) 274–319.
[9] J. Gang, J.P. Morniroli, T. Grosdidier, Scripta Mater. 48 (2003) 1599–1604.

[10] M. Omori, Mater. Sci. Eng. A 287 (2000) 183–188.
[11] T. Grosdidier, G. Ji, F. Bernard, E. Gaffet, Z.A. Munir, S. Launois, Intermetallics 14 (2006) 1208–1213.
[12] Y.M. Wang, E. Ma, Acta Mater. 52 (2004) 1699–1709.
[13] Y.M. Wang, M.W. Chen, F.H. Zhou, E. Ma, Nature 419 (2002) 912–915.
[14] X. Zhang, H. Wang, R.O. Scattergood, J. Narayan, C.C. Koch, A.V. Sergueeva, A.K. Mukherjee, Acta Mater. 50 (2002) 4823–4830.
[15] B.Q. Han, E.J. Lavernia, Adv. Eng. Mater. 7 (2005) 457–465.
[16] T. Grosdidier, G. Ji, S. Launois, Scripta Mater. 57 (2007) 525–528.
[17] N. Kamikawa, X. Huang, N. Hansen, J. Mater. Sci. 43 (2008) 7313–7319.
[18] J.W. Christian, S. Mahazan, Prog. Mater. Sci. 39 (1995) 1–157.
[19] L. Lu, Y.F. Shen, X.H. Chen, L.H. Qian, K. Lu, Science 304 (2004) 422–426.
[20] L. Lu, R. Schwaiger, Z.W. Shan, M. Dao, K. Lu, S. Suresh, Acta Mater. 53 (2005) 2169–2179.
[21] Y.F. Shen, L. Lu, Q.H. Lu, Z.H. Jin, K. Lu, Scripta Mater. 52 (2005) 989–994.
[22] K. Lu, J. Lu, Mater. Sci. Eng. A 375–377 (2004) 38–45.
[23] K. Lu, J. Lu, J. Mater. Sci. Technol. 15 (1999) 193–197.
[24] K. Wang, N.R. Tao, G. Liu, J. Lu, K. Lu, Acta Mater. 54 (2006) 5281–5291.
[25] N.R. Tao, X.L. Wu, M.L. Sui, J. Lu, K. Lu, J. Mater. Res. 19 (2004) 1623–1629.
[26] K.Y. Zhu, A. Vassel, A. Brisset, K. Lu, J. Lu, Acta Mater. 52 (2004) 4101–4110.
[27] G. Liu, S.C. Wang, X.F. Lou, J. Lu, K. Lu, Scripta Mater. 44 (2001) 1791–1795.
[28] N.R. Tao, Z.B. Wang, W.P. Tong, M.L. Sui, J. Lu, K. Lu, Acta Mater. 50 (2002) 4603–4616.
[29] H.W. Zhang, Z.K. Hei, G. Liu, J. Lu, K. Lu, Acta Mater. 51 (2003) 1871–1881.
[30] X.H. Chen, J. Lu, L. Lu, K. Lu, Scripta Mater. 52 (2005) 1039–1044.
[31] A.A. Rasmussen, J.A.D. Jensen, A. Horsewell, M.A.J. Somers, Electrochim. Acta 47 (2001) 67–74.
[32] V.M. Kozlov, L.P. Bicelli, Mater. Chem. Phys. 77 (2002) 289–293.
[33] B. Hong, C.H. Jiang, X.J. Wang, Surf. Coat. Technol. 201 (2007) 7449–7452.